European Journal of Orthodontics 21 (1999) 15–29

Morphological changes in periodontal mechanoreceptors of mouse maxillary incisors after the experimental induction of anterior crossbite: a light and electron microscopic observation using immunohistochemistry for PGP 9.5

T. Piyapattamin*, Y. Takano**, K. Eto*** and K. Soma*
*First Department of Orthodontics, **Second Department of Oral Anatomy and ***Department of Developmental Biology, Tokyo Medical and Dental University, Japan

SUMMARY Ruffini nerve endings (mechanoreceptors) in the periodontal ligament (PDL) of mouse incisors were examined to elucidate whether experimentally-induced crossbites cause any changes or abnormalities in their morphology and distribution. Anterior guiding planes were attached to the mandibular incisors of 3-week-old C3H/HeSlc mice. At 3 days and 1, 2, 4, 6, and 8 weeks post-attachment of the appliance, the mice were sacrificed by perfusion fixation. Frozen sagittal cryostat sections of the decalcified maxillary incisors were processed for immunohistochemistry of protein gene product 9.5, followed by histochemical determination of tartrate-resistant acid phosphatase activity to reveal sites of alveolar bone resorption.

Despite the absence of bone resorption within the lingual PDL of control mice, distinct resorption sites were seen in the respective regions of the experimental animals. Unlike the controls, many Ruffini endings showing vague and swollen contours, with unusually long and pedunculated micro-projections were observed in the affected lingual PDL of the incisors in the experimental animals with short-term anterior crossbite induction. Club-shaped nerve terminations with few, if any, micro-projections were observed in the lingual PDL of experimental animals with long-term induction, as well as in aged control mouse incisors. Differences in the distribution of Ruffini endings were also observed. These results indicate that changing the direction of the force applied to the PDL results in rapid and prolonged changes in the morphology of Ruffini-like mechanoreceptors.

Introduction

Anterior crossbite of one or two teeth can develop even in children with good facial proportions (Proffit and Fields, 1993), and is common in patients with mandibular dysfunction (Mohlin and Kopp, 1978; Egermark-Eriksson *et al.*, 1983). Crossbites can affect chewing patterns in humans (Kitamura *et al.*, 1987) and cause a functional anterior shift of the mandible, leading to muscle pain which almost always correlates with a history of holding the mandible in an anterior or lateral position (Proffit, 1993).

Periodontal mechanoreceptors are involved in the induction of various oral reflexes, which make regular and smooth mastication possible (Matthews, 1975; Linden, 1990). Recent electrophysiological studies have shown that there is only one type of periodontal mechanoreceptor (Cash and Linden, 1982; Linden and Millar, 1988; Linden *et al.*, 1994) and Ruffini endings are found in the periodontal ligament (PDL) in all mammals (Linden *et al.*, 1995). Rodent incisors continuously erupt and are worn at the incisal edge by attrition throughout life, which makes

them useful for studies of dental histogenesis (Schour and Massler, 1962; Rugh, 1967). The presence and distribution of Ruffini endings in the lingual PDL of mouse maxillary incisors (Sato *et al.*, 1989) have been shown to be similar to those in rat maxillary incisors, whose normal structure and distribution of Ruffini endings have been confirmed (Sato *et al.*, 1988; Maeda *et al.*, 1989).

Protein gene product 9.5 (PGP 9.5) is a general marker for nerve and neuroendocrine cells (Schmechel *et al.*, 1978; Thompson *et al.*, 1983; Ramieri *et al.*, 1990), and recent immunohistochemical research has shown that anti-PGP 9.5 antibody is useful for demonstrating nerve elements in post-natal developing dental structures (Fristad *et al.*, 1994), and particularly Ruffini endings in the PDL (Nakakura *et al.*, 1993, 1995).

Resorption and apposition occur physiologically in bone that has adapted to mechanical stress (Bhaskar, 1986). Both processes are generally induced during orthodontic treatment; the former characterizes the pressure side of the PDL, whereas the latter the tension side (Reitan, 1985). Osteoclasts, which are associated with areas of bone resorption (Minkin, 1982; Lee *et al.*, 1995; Urena *et al.*, 1996), can be detected by histochemistry for tartrate-resistant acid phosphatase (TRAP) activity using the azo dye technique (Tsuchiya *et al.*, 1995).

Kamata (1994) showed that the responses of the motor unit (RMU) in the contralateral temporal muscle to the direction of mechanical stimulation applied to the tooth varied between subjects with normal occlusion and those with crossbite. This difference in the RMU of the masticatory muscles between subjects with normal occlusion and those with crossbite may depend on the distribution of periodontal mechanoreceptors for the respective teeth. The purpose of this study was to clarify whether there were any changes or abnormalities in the morphology and distribution of Ruffini endings in the PDL of mouse incisors following short- and long-term induction of anterior crossbite by immunohistochemistry for PGP 9.5 and histochemistry for acid phosphatase activity using light and electron microscopy.

Materials and methods

Animals

C3H/HeSlc mice, 3 weeks of age, were used in this study. An anterior guiding plane appliance constructed from band material (0.125×0.003 inch; Rocky Mountain, USA) was attached to their mandibular incisors using methylmethacrylate (Super Bond: Sun Medical Co. Ltd., Kyoto, Japan). Untreated mice were used as controls. The eating, drinking, and grooming behaviour of the mice was monitored throughout the experimental periods. The treated mice ($n = 6$ for each group), together with their controls ($n = 6$ for each group), were killed at 3 days and 1, 2, 4, 6, and 8 weeks post-attachment of the appliance, and control mice were additionally killed 10, 12, 14, and 16 weeks post-attachment ($n = 6$ for each group). Prior to death, radiographic images of the mice in both groups were taken using a Hitachi DH-158 HM camera (Hitachi Co. Ltd., Tokyo, Japan; 43 kV, 400 mAs and 112-cm focus film). The mice were deeply anaesthetized with diethyl ether and intracardially perfused with 4 per cent paraformaldehyde in 0.1 M phosphate buffer (PB), pH 7.4. Their maxillae were then removed, immersed *en bloc* in the same fixative solution at 4°C for 14 hours, and decalcified in 10 per cent ethylene diamine tetra-acetic acid (EDTA)-2Na solution, pH 7.4, at 4°C for 3 weeks. The decalcified tissues were saturated overnight in 30 per cent sucrose solution at 4°C.

Frozen sections, 20–30 μm thick, were cut serially and sagittally using a cryostat (Leica CM3000, Nussloch, Germany), mounted on poly-L-lysine-coated glass slides (Matsunami, Osaka, Japan), and processed using the avidin-biotin-complex (ABC) method. Free-floating 50-μm thick sections were also prepared for electron microscopic observation.

Light microscopic immunohistochemistry and histochemistry

Anti-PGP 9.5 antibody, which directly recognizes the cytoplasmic protein contained in central and peripheral neurons, was used for the immunohistochemical visualization of nerve elements.

The origin and characterization of rabbit polyclonal anti-human PGP 9.5 antibody (Ultraclone Co. Ltd., Cambridge, UK) used as the primary antibody in this study have been verified by Doran *et al.* (1983), Thompson *et al.* (1983), and Gulbenkian *et al.* (1987).

Prior to immunohistochemical incubation of the cut sections with the primary antibody, endogenous peroxidase, and non-specific immunoreactivity, respectively, were inactivated with 0.3 per cent H_2O_2 in absolute methanol for 30 minutes, and then with 2 per cent normal goat serum (Vector Laboratories, Burlingame, CA, USA) in 0.01 M phosphate-buffered saline (PBS), pH 7.4. The sections were then incubated overnight at 37°C with the primary antibody (dilution 1:10 000), and then with biotinylated anti-rabbit IgG (Chemicon, CA, USA) and ABC complex, according to the manufacturers' instructions (Vector Laboratories, Burlingame, CA, USA). At each step, the sections were washed several times in 0.01 M PBS containing 0.3 per cent Triton X-100 (Sigma Chemical, St Louis, MO, USA).

After treatment by the ABC method, histochemistry for TRAP activity was performed using the azo dye technique, as previously described by Tsuchiya *et al.* (1995). Briefly, the staining solution consisted of naphthol 3-hydroxy-2-naphtho-2,4-xylidide (AS-MX) phosphate sodium salt (Sigma) as the substrate, fast red violet 5-chloro-4-benzamido-2-methylbenzenediazonium chloride, hemi (zinc chloride) (LB) salt (Sigma) as the diazonium salt, and 50 mM l(+)-tartric acid (Wako Pure Chemical Industries, Tokyo, Japan) as the inhibitor of acid phosphatase for TRAP activity. Incubation was conducted at 37°C for 12 minutes and at pH 5.3 with an acetate buffer.

For the final visualization of immunoreactive sites, sections that had already been incubated for TRAP activity were treated with 0.02 per cent 3,3-diaminobenzidine tetrahydrochloride and 0.01 per cent H_2O_2 in 0.05 M Tris–HCl buffer, pH 7.6. The sections were then counterstained with 1 per cent methyl green, dehydrated in graded ethanol, rinsed in xylene, and finally mounted with Entellan new (E. Merck, Darmstadt, Germany).

Electron microscopic immunohistochemistry and histochemistry

Floating 50-μm thick sections were processed for PGP 9.5 immunohistochemistry and TRAP histochemistry as described above, except that pre-treatment with 0.3 per cent H_2O_2 in absolute methanol, Triton X-100, and counterstaining were omitted. After light microscopic observation and photography, sections were post-fixed with 2 per cent glutaraldehyde in 0.1 M PB, pH 7.4, for 2 hours, and then with 1 per cent osmium tetroxide (OsO_4) reduced with 1.5 per cent potassium ferrocyanide in the same buffer for 2 hours. The sections were then dehydrated in graded ethanol and flat-embedded in Epon 812. Ultra-thin sections were cut with a diamond knife, double-stained with uranyl acetate, and Reynold's lead solution, and examined under a Hitachi H-800 transmission electron microscope (Hitachi Co. Ltd., Tokyo, Japan) at an accelerating voltage of 75 kV.

For ultrastructural observation, some mice were similarly perfused with a mixture of 3 per cent paraformaldehyde and 2.5 per cent glutaraldehyde in 0.1 M PB, pH 7.4, followed by EDTA decalcification, OsO_4 post-fixation, and embedding in Epon 812.

Specificity controls

To check the specificity of the immunoreactions, the primary antibody was replaced with non-immune rabbit serum or treatment with anti-rabbit IgG or ABC complex was omitted.

Evaluation of the direction of occlusal force and quantitative analysis of histological sections

To identify the sites at which compressive force was applied in tooth-facing alveolar bone, the distribution of TRAP-positive cells was evaluated in the marginal, middle, and basal areas of the labial and lingual PDL. The horizontal length from the labial or lingual alveolar bone tips to the apical growing ends of dentine on the respective sides was divided into three segments of equal length, designated as area I (marginal third), area II (middle third), and area III (basal third) as shown in Figure 10. In addition, a pixel

image analysis was carried out to quantify the histological changes in Ruffini endings in the lingual PDL, and the following parameters were measured:

(1) the sectional surface area of the lingual PDL (Table 1);
(2) the surface area occupied by abnormal Ruffini endings with swollen and hazy contours as a percentage of the total lingual PDL surface (Table 2);
(3) the surface area occupied by abnormal club-shaped Ruffini endings as a percentage of the total lingual PDL surface (Table 3).

For the surface analysis, five sections were randomly selected per animal ($n = 6$ for each control and for each treated group). Photographic slides of the sections were converted into digital images at a resolution of 1 200 pixels per inch at a scan pitch of 2 pixels. The surface within the described area was measured using image-analysis software (Image version 1.55, provided by NIH) and the data were expressed in terms of the number of pixels. Since nerve endings had been immunohistochemically stained dark-brown, the image was first converted to cyano-magenta-yellow, black for colour separation to leave only stained nerves. The areas occupied by the apparently abnormal nerve elements described in (2) and (3) were analysed. The total PDL surface area was obtained by selecting 16 colour gradients within the white-to-light yellow range and subsequent erasure of remaining unwanted non-PDL tissue. The percentage of the surface area occupied by club-shaped Ruffini endings or those with swollen and hazy contours was then calculated as: $100 \times$ number of pixels occupied by the respective nerve endings/number of pixels occupied by the lingual PDL.

All measurements were performed blind by three observers and in duplicate. The numerical data obtained were examined by an analysis of variance (ANOVA) and *post hoc* comparisons were made using the Newman–Keuls (NK) test. A probability value of less than 5 per cent ($P < 0.05$) was considered significant.

Results

Although both the treated mice and controls gained weight during the experimental period (1.38 ± 3.71 g/week and 1.30 ± 3.38 g/week, respectively; mean ± standard deviation), there was no significant difference between the two groups (Table 4). ANOVA showed that age, but not treatment, affected body weight. In addition, the interaction of these two factors did not affect mouse body weight. *Post hoc* comparisons by the NK test indicated that there were significant differences in the mean body weight at each developmental stage (Figure 1).

Specificity controls of immunohistochemistry for PGP 9.5 showed no immunolabelling. The immunoreactive sites in this study did not exhibit any interference between the two reactions, i.e. immunohistochemistry for PGP 9.5 and subsequent histochemistry for TRAP activity, which indicates that both nerve elements and TRAP-positive areas differed between the treated groups and controls.

Time-related changes in occlusion

Radiographic images showed that by 2 weeks post-attachment of the appliance, the maxillary incisors of the treated groups, versus those of the controls (Figure 2a), were curved intraorally, resulting in a crossbite in relation to the mandibular incisors (Figure 2b). As the experimental period was prolonged, the maxillary incisors became spiral in shape and the anterior crossbite relationship was more pronounced (Figure 2c). The tips of the maxillary incisors did not touch the palatal mucous membrane by the time the animals were killed and no visible inflammatory change in the oral tissue was observed.

Histochemistry for TRAP activity

Histological sections from controls (Figure 3a) stained for TRAP activity with the azo dye technique showed the same pattern of osteoclast distribution; i.e. osteoclasts extended from the labial to the lingual epithelial diaphragm around the basal end, and from the marginal to the

Table 1 Surface area of lingual PDL of the anterior crossbite induced maxillary incisors in comparison with their controls. (All values are expressed in mean ± standard deviation pixels of five sections per animal; $n = 6$ for each control and treated group.)

	0 day	3 days	1 week	2 weeks	4 weeks	6 weeks	8 weeks
Marginal third							
Control	5671.13 ± 705.51	6154.33 ± 1008.84	6244.44 ± 769.46	6191.11 ± 565.30	6923.70 ± 407.76	6624.24 ± 554.24	6790.16 ± 462.89
Crossbite	ND	5049.63 ± 477.30	5256.49 ± 365.30	4966.51 ± 316.69	5680.37 ± 376.88	3671.11 ± 361.00**	3519.51 ± 338.63**
Middle third							
Control	4650.19 ± 368.58	5080.00 ± 694.36	5392.01 ± 778.24	5580.17 ± 337.44	5992.28 ± 363.87	5847.62 ± 599.00	6014.84 ± 459.46
Crossbite	ND	5600.35 ± 614.76▲	6218.51 ± 276.14*▲	6161.28 ± 605.16▲	6844.11 ± 254.20*▲	6420.5 ± 527.27	7084.85 ± 532.46*▲
Basal third							
Control	5168.19 ± 423.7	5340.01 ± 356.33	6018.18 ± 453.56	5861.45 ± 360.05	5422.23 ± 485.86	5614.75 ± 310.31	5862.48 ± 357.35
Crossbite	ND	5836.28 ± 445.99*▲	6547.43 ± 260.58*▲	6849.13 ± 490.04**▲	5948.27 ± 377.66*▲	6817.13 ± 318.81**▲	6641.19 ± 378.23*▲

*Difference between control and treated teeth for the respective area significant at $P < 0.05$.
**Difference between control and treated teeth for the respective area significant at $P < 0.001$.
▲ Intragroup difference significant at $P < 0.001$.
ND: not determined.

Table 2 Percentage of surface area occupied by the swollen and hazy contoured nerve endings in relation to the total PDL surface between anterior crossbite induced teeth and their controls. (All values are expressed in mean ± standard deviation pixels of five sections per animal; $n = 6$ for each control and each treated group.)

	0 day	3 days	1 week	2 weeks	4 weeks	6 weeks	8 weeks
Marginal third							
Control	0.02 ± 0.02	0.01 ± 0.01	0.03 ± 0.03	0.01 ± 0.01	0.02 ± 0.01	0.01 ± 0.01	0.05 ± 0.04
Crossbite	ND	0.10 ± 0.02*▲	0.13 ± 0.05*▲	0.13 ± 0.03*▲	0.19 ± 0.03*▲	0.20 ± 0.04*▲	0.14 ± 0.03*▲
Middle third							
Control	0.10 ± 0.08	0.11 ± 0.06	0.13 ± 0.04	0.14 ± 0.06	0.10 ± 0.02	0.14 ± 0.03	0.17 ± 0.07
Crossbite	ND	0.53 ± 0.07*▲	0.37 ± 0.03*▲	0.65 ± 0.05*▲	0.70 ± 0.03*▲	0.51 ± 0.03*▲	0.44 ± 0.03*▲
Basal third							
Control	0.08 ± 0.01	0.04 ± 0.01	0.10 ± 0.08	0.13 ± 0.03	0.09 ± 0.04	0.11 ± 0.03	0.13 ± 0.02
Crossbite	ND	0.47 ± 0.06*▲	0.32 ± 0.03*▲	0.58 ± 0.06*▲	0.62 ± 0.03*▲	0.57 ± 0.04*▲	0.38 ± 0.04*▲

*Difference between control and treated teeth for the respective area significant at $P < 0.001$.
▲ Intragroup difference significant at $P < 0.001$.
ND: not determined.

Table 3 Percentage of surface area occupied by the club-shaped nerve endings in relation to the total PDL surface between anterior crossbite induced teeth and their controls. (All values are expressed in mean ± standard deviation pixels of five sections per animal; $n = 6$ for each control and each treated group.)

	0 day	3 days	1 week	2 weeks	4 weeks	6 weeks	8 weeks	10 weeks	12 weeks	14 weeks	16 weeks
Marginal third											
Control	ND	UO	UO	UO	UO	0.02 ± 0.01	0.04 ± 0.01	0.01 ± 0.01	0.06 ± 0.02	0.02 ± 0.01	0.05 ± 0.04
Crossbite	ND	UO	UO	UO	0.04 ± 0.01	0.03 ± 0.02*△	0.06 ± 0.02**△	ND	ND	ND	ND
Middle third											
Control	ND	UO	UO	UO	UO	0.17 ± 0.04	0.38 ± 0.05	0.52 ± 0.02	0.46 ± 0.03	0.45 ± 0.04	0.57 ± 0.03
Crossbite	ND	UO	UO	UO	0.63 ± 0.05	0.58 ± 0.02**▲	0.9 ± 0.04**▲	ND	ND	ND	ND
Basal third											
Control	ND	UO	UO	UO	UO	0.06 ± 0.02	0.05 ± 0.02	0.02 ± 0.01	0.05 ± 0.02	0.06 ± 0.01	0.1 ± 0.02
Crossbite	ND	UO	UO	UO	0.09 ± 0.03	0.12 ± 0.03**▲	0.19 ± 0.03**▲	ND	ND	ND	ND

*Difference between control and treated teeth for the respective area significant at $P < 0.05$.
**Difference between control and treated teeth for the respective area significant at $P < 0.001$.
△ Intragroup difference significant at $P < 0.05$, ▲ Intragroup difference significant at $P < 0.001$.
ND: not determined; UO: unobservable.

Table 4 Body weight (g) of mice during the experimental periods in comparison with their controls. (All values are expressed in mean ± standard deviation.)

Weeks	Treated groups	Untreated controls
0	11.37 ± 0.16	12.50 ± 0.08
1	14.68 ± 0.24	14.12 ± 0.19
2	18.28 ± 0.14	18.78 ± 0.25
3	21.58 ± 1.11	21.15 ± 0.08
4	21.57 ± 0.82	20.13 ± 1.03
5	21.33 ± 1.06	20.58 ± 0.24
6	22.90 ± 0.33	21.88 ± 0.93
7	20.90 ± 1.14	21.40 ± 0.06
8	22.37 ± 1.29	22.87 ± 0.37

middle third of tooth-facing labial alveolar bone (Figure 3a, arrowheads). No osteoclasts were found in tooth-facing lingual alveolar bone in any of the controls.

In the treated groups (Figure 3b), osteoclasts around the basal end showed a distribution similar to that in the controls. In tooth-facing labial alveolar bone, they were restricted to a narrow area between the middle and basal thirds (Figure 3b, arrowheads on the labial side). In tooth-facing lingual alveolar bone, they were found within the marginal third of the PDL (Figure 3b, arrowheads on the lingual side). Together with a reduced lingual PDL width (Figure 1a–c and Table 2), numerous resorptive lacunae were observed in the marginal third.

Immunohistochemistry for PGP 9.5

Control groups. Thick nerve bundles showing PGP 9.5 immunoreactivity entered the lingual PDL through slits in the lingual bone (Figure 4a). Some of these nerve bundles branched toward the marginal (Figure 4d) and basal thirds (Figure 4b), and began to ramify in a dendritic manner. Each branch terminated in an expanded feature which was regarded as a Ruffini ending, was intimately associated with periodontal collagenous fibres, and was restricted to the alveolus-related part of the PDL. The Ruffini endings were concentrated in the middle region of the lingual PDL (Figures 1d–f, and 4c, and Table 3). The marginal third, compared with the other regions of the lingual PDL, contained fewer nerve endings (Figure 1d–f and Table 2). At high magnification, Ruffini endings possessed irregular outlines with numerous fine micro- or finger-like projections (Figure 5a). Thin ramified nerve fibres, without any expanded terminations (Figure 5b), were also seen at high magnification.

Ultrastructural observation (Figure 6a) revealed that Ruffini endings consisted of expanded axon terminals filled with numerous mitochondria. The axon terminals were covered by thick Schwann sheaths. They were further surrounded by several layers of basal lamina, which were penetrated by collagenous fibrils. Multiple finger-like projections (Figure 6b,c, arrows) or axonal spines extended from the axon terminals through slits in the Schwann sheath.

In the PDL of control mice aged 9 weeks and older, new lingual alveolar bone was apposed to the direction of the cementum, causing the previously formed alveolar bone (area under the dotted line in Figure 7a) to be left under the newly-formed bone (area above the dotted line in Figure 7a). The area over the newly-formed alveolar bone contained well-developed Ruffini endings with the previously recognized features (Figure 7b). In the PDL of 19-week-old control mice, some of the Ruffini endings were sandwiched between the old and new alveolar bone areas. Such nerve endings, which were isolated from the functioning PDL areas, possessed a club-shaped morphology with a smooth outline (Figure 7c). Immuno-electron microscopic observation of these club-shaped Ruffini endings revealed a marked reduction in the number of mitochondria and other cytoplasmic organelles (Figure 7d).

Treated groups. The nerve structure and distribution in the treated groups were different from those in the controls. On day 3 post-attachment of the appliance, the Ruffini endings with expanded terminations were more swollen with vague contours, compared with those in the controls (Figure 8a). Numerous micro-projections with extremely long stalks and clearly different shapes from those in the controls were easily recognized (Figure 8b,c). Such

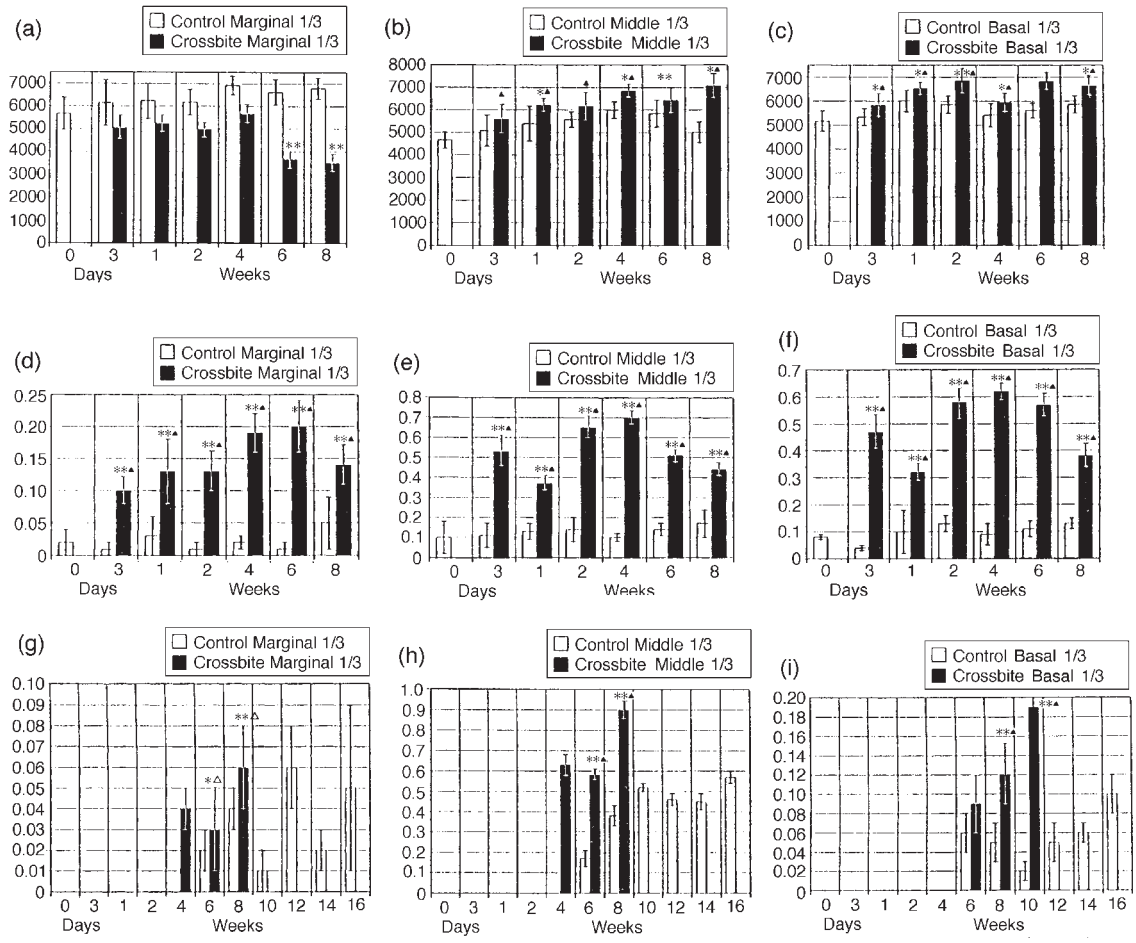

Figure 1 Differences (mean ± standard deviation denoted by error bars) in the surface area of the lingual periodontal ligament (PDL) (a–c), the percentage of the total lingual PDL surface area occupied by abnormally swollen and hazy-contoured nerve endings (d–f), and the percentage of the total lingual PDL surface area occupied by club-shaped nerve endings (g–i) between teeth in which anterior crossbite was induced and controls. *, Intergroup difference significant at $P < 0.05$; **, intergroup difference significant at $P < 0.001$; △, intragroup difference significant at $P < 0.05$; ▲, intragroup difference significant at $P < 0.001$.

Figure 2 Lateral skull radiographs showing the relationship between the maxillary and mandibular incisors of mice. (a) Control; (b) 2 weeks post-attachment of the appliance; (c) 8 weeks post-attachment.

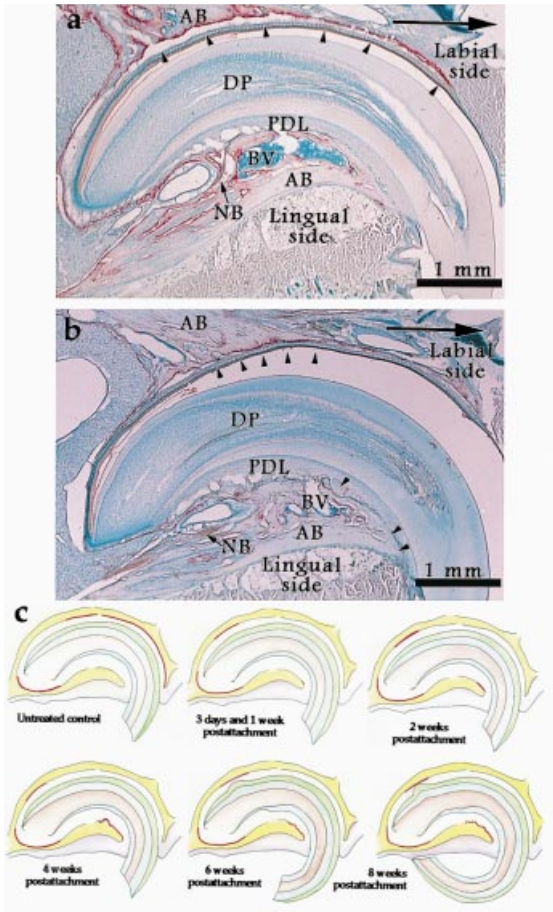

Figure 3 (a,b) Histochemical reactions (red) for TRAP activity using the azo dye technique in sagittally cut frozen sections of the PDL of mouse maxillary incisors. (a) Control. Osteoclasts (arrowheads) extend from the marginal third to the middle third in tooth-facing labial alveolar bone (AB). No osteoclasts were seen in tooth-facing lingual alveolar bone. (b) Three days post-attachment of the appliance. Note the difference in the location of osteoclasts compared with (a) in that they are restricted to within a narrow area (arrowheads on the labial side) between the middle and basal thirds of labial alveolar bone. Osteoclasts in the resorptive lacunae (arrowheads on the lingual side) are also in the marginal third of tooth-facing lingual alveolar bone. BV, blood vessel; DP, dental pulp; NB, nerve bundle. Note the PGP 9.5 immunoreactions (brown) of the neural elements. Large arrows in these and subsequent figures indicate the direction of the incisal edge. Methyl green counterstaining, ×5. (c) Areas where histochemical reactions for TRAP activity (red marks) were observed in the control and treated groups.

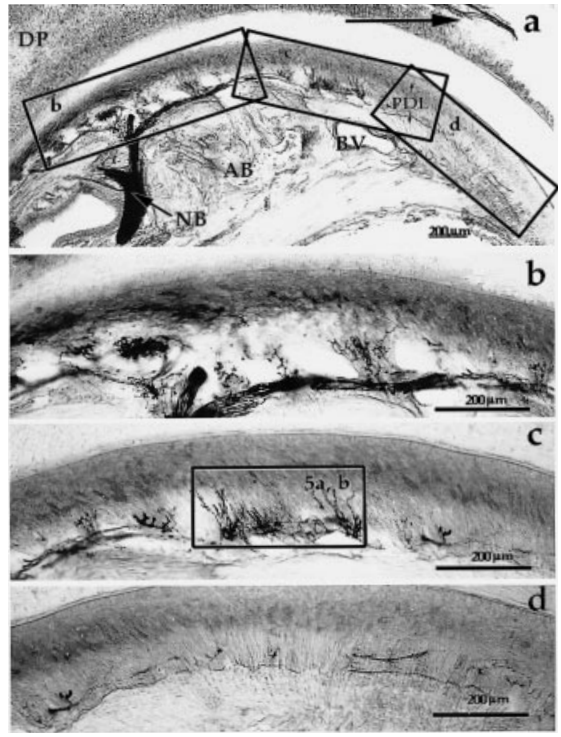

Figure 4 (a–d) Distribution of PGP 9.5-immunoreactive nerve elements in the lingual PDL of the incisor of a 7-week-old control mouse. (a) A thick nerve bundle (NB) enters the lingual PDL through the alveolar bone slit and branches toward the basal and marginal thirds. Note that the basal (4b) and middle thirds (4c), in comparison with the marginal third (4d), are enriched with nerve endings. Figure b, c, and d show the respective areas in Figure 4a. AB, alveolar bone; BV, blood vessel; DP, dental pulp. (a) ×10; (b), (c), and (d) ×25.

Ruffini endings with swollen and hazy contours were distributed throughout the lingual PDL (Figure 1d–f and Table 2). Compared with those in the controls, the swollen axonal spines possessed longer pedunculated stalks that did not contain organelles (Figure 8d).

Four weeks after the induction of anterior crossbite, club-shaped Ruffini endings were observed in the middle region of the alveolus-related part of the lingual PDL (Figures 1g–i and 9a, and Table 3). Neither newly-formed nor resorbed alveolar bone was observed in this area. Micro-projections from the axon terminals were either partially reduced (Figure 9a, magnified

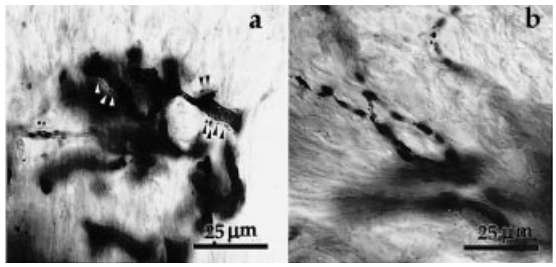

Figure 5 (a,b) Higher magnification of the boxed area in Figure 4c illustrating the structure of PGP 9.5-immunoreactive nerve elements in the lingual PDL of the incisor of a 7-week-old control mouse. (a) Ruffini-like endings possessing irregular outlines with fine micro-projections (arrowheads). (b) Thin ramified nerves without any expanded terminations. ×250.

boxes) or completely absent (Figure 9b,c), causing their structures to be similar to those in old-aged control mice. The marginal and basal thirds of the lingual PDL contained Ruffini endings whose structures were similar to those observed in the treated mice in the earlier stages (Figure 1d–f and Table 2). Immuno-electron microscopy revealed that the club-shaped Ruffini endings had the same structures as those observed in older control mice.

Discussion

The results of this study indicate a clear difference in PGP 9.5-immunoreactive neural elements situated in the lingual PDL of mouse maxillary incisors between experimentally induced anterior crossbite and controls.

The chewing cycle of rats (Hiiemäe, 1967) begins with a preparatory stage, in which the mandibular incisors are moved to below and slightly behind the maxillary incisors. This is followed by an incisive stage, in which the mandibular incisal edges are brought into an edge-to-edge relationship with the maxillary incisors to sever a particle of food or to bite. The latter stage is rapidly repeated several times in a chopping or chiselling motion until the

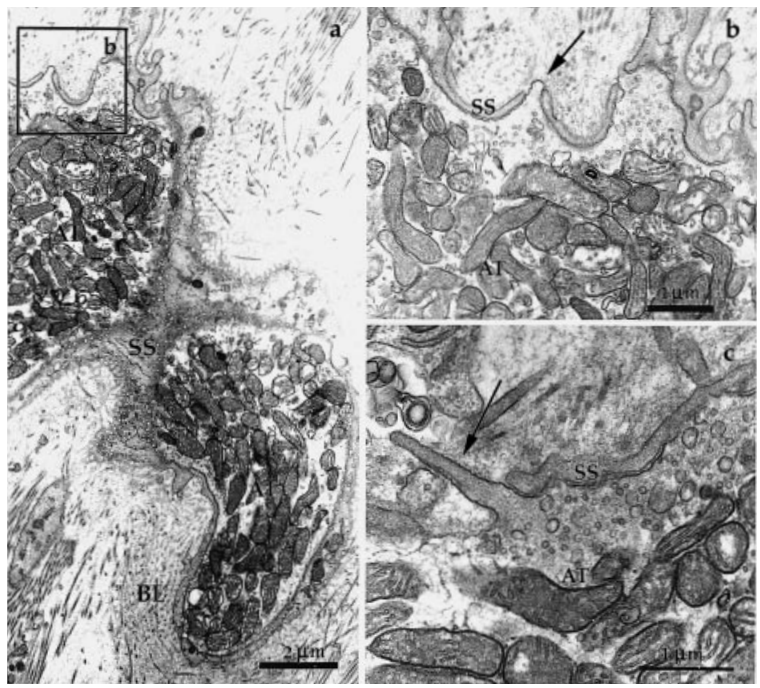

Figure 6 (a–c) Ultrastructure of typical Ruffini endings in the incisor PDL of a 5-week-old control mouse. (a) Axon terminals (AT) filled with numerous mitochondria are surrounded by a thick Schwann sheath (SS) and multiple layers of basal lamina (BL). (b) Higher magnification of the boxed area in Figure 6a showing an axonal spine or finger-like projection (arrow) which extends from the axon terminal through a slit in the Schwann sheath. (c) Another typical finger-like projection (arrow). (a) ×7320; (b) ×12 810; (c) ×17 080.

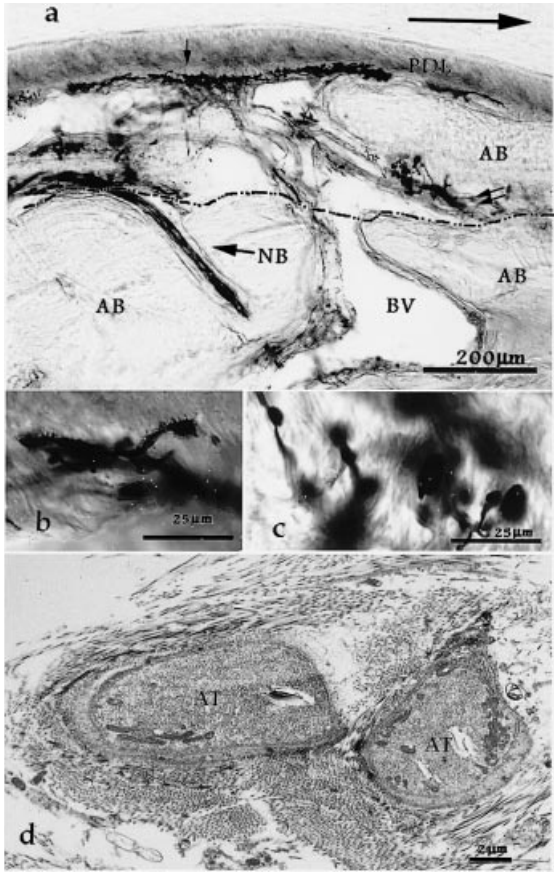

Figure 7 (a–d) Distribution and structure of PGP 9.5-immunoreactive nerve elements in the lingual PDL of the incisor of a 19-week-old control mouse. (a) The previously formed alveolar bone (AB, area under the dotted line) is left underneath the newly-formed bone (AB, area above the dotted line). (b) Higher magnification of the Ruffini-like endings (small single arrow in Figure 7a) near the new alveolar bone possessing an irregular outline with fine micro-projections, as previously observed. (c) Higher magnification of Ruffini-like endings (small double arrows in Figure 7a) trapped between the new and old alveolar bone areas. These possess a club-shaped morphology and a smooth outline. (d) Immuno-electron microscopic view of the club-shaped Ruffini endings shown in Figure 7c. Note the marked reduction in the number of mitochondria and other organelles within the axon terminals (AT). BV, blood vessel; NB, nerve bundle. (a) ×50; (b), (c) ×200, (d) ×6210.

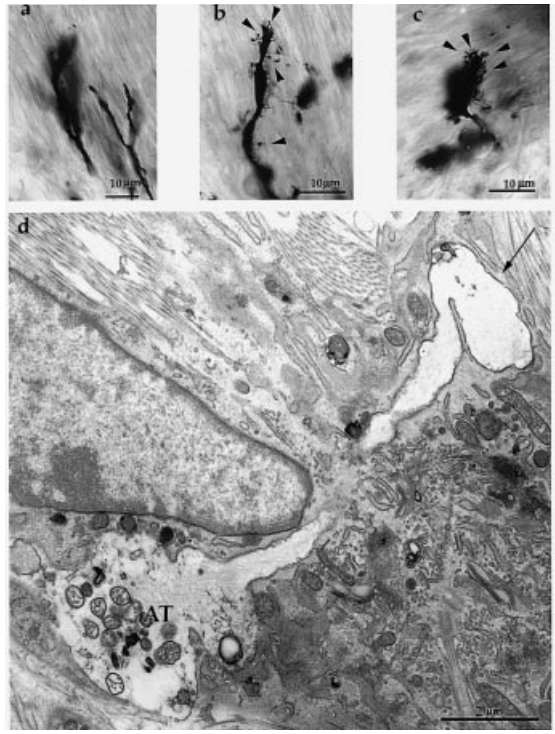

Figure 8 (a–d) Nerve endings in the experimental group 3 days post-attachment of the appliance. (a) Relatively thin and hazy outlined endings. (b) Ruffini-like endings possessing numerous micro-projections whose stalks are extremely long and easily detected (arrowheads). (c) Ruffini-like endings possessing numerous micro-projections (arrowheads) with visible stalks. Note the difference in the number, size, and structure of the micro-projections observed here and those in Figures 5a and 7b. (d) Ultrastructure of Ruffini endings in the experimental group (2 weeks post-attachment of the appliance). The swollen axonal spine (arrow) extending from the axon terminal (AT) possesses an unusually long stalk, compared with those in the control. Compare the pedunculated shape of the axonal spine in this figure with the finger-like extensions of those in Figures 6b, c. (a) ×250; (b) and (c) ×360; (d) ×6210.

mandibular incisal edge is removed from the body of the food and the stroke is carried to completion. In this study, TRAP histochemical results showed that most of the labial alveolar bone of the control mice was on the pressure side, since it contained osteoclasts and resorptive lacunae. In old-aged control mice, new alveolar bone is formed in the lingual portion, which causes old alveolar bone to be left underneath the new bone. The lingual PDL of control mice

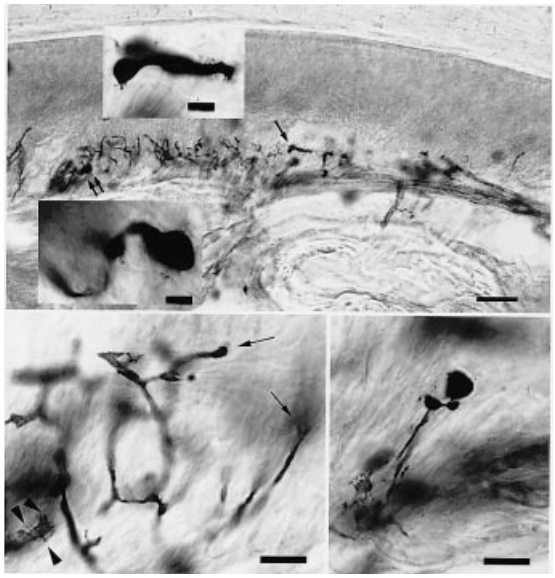

Figure 9 (a–c) Distribution and structure of nerve endings in the lingual PDL observed in the experimental group (4 weeks post-attachment of the appliance). (a) Despite no newly-formed alveolar bone (AB), the middle region of the lingual alveolar bone contains club-shaped Ruffini-like endings. The upper magnified box in (a) shows club-shaped Ruffini-like endings (small arrow) with some micro-projections (arrowheads), while the lower box shows club-shaped Ruffini-like endings (small double arrows) with fewer micro-projections. (b) Co-existence of club-shaped Ruffini-like endings (small arrows) and regular-shaped endings with long and clear micro-projections (arrowheads). (c) Club-shaped nerve ending with a smooth outline. (a) ×50; (b) and (c), magnified boxes in (a) ×250.

can thus be assumed to be on the tension side, since the apposition of bone characterizes the tension side (Reitan, 1985). In a lateral skull radiograph, masticatory force appears to cause a counter-clockwise rotation of the maxillary incisors, and the rotation axis is situated somewhere within the lingual alveolar bone (Figure 10a).

To the best of our knowledge, this is the first report of club-shaped Ruffini endings in old-aged mouse incisor PDL. Kvinnsland and Kvinnsland (1990) observed club-shaped nerve terminals that were immunoreactive to calcitonin gene-related peptide (CGRP) antibody in rat molar PDL during experimental tooth movement. However, Ruffini endings display no immunoreactivity for CGRP (Kato *et al.*, 1992). Therefore, it is possible that the club-shaped nerve terminals visualized in their study were not Ruffini endings. On the other hand, those observed in this study were apparently the extension of typical Ruffini endings, implying that they are a modified structure of this type of nerve ending.

The PDL of mouse maxillary incisors is distorted in accordance with the mechanical force applied to the tooth, and its lingual portion is thought to be stretched during mastication. Histologically, the lingual PDL consists of a moving, tooth-related part and a non-moving, alveolus-related part (Beertsen, 1975; Shore and Berkovitz, 1978). Moreover, recent studies have shown that Ruffini endings are located only in the latter part (Sato *et al.*, 1988, 1989; Maeda *et al.*, 1989, 1991; Nakakura *et al.*, 1993, 1995). Compared with those observed previously, the club-shaped Ruffini endings in the PDL of old-aged control mouse incisors in this investigation were in a distinct location; i.e. sandwiched between old and new, more lingually-deposited alveolar bone. The newly-formed alveolar bone may hinder masticatory force, which is transferred to where the club-shaped Ruffini endings are located. Malathi and Batmanabane (1983) showed that immobilization of a cat hind limb causes a reduction in the mean fibre diameter of the nerve supplying the gastrocnemius muscle, and that prolonged immobilization beyond 8 weeks results in splitting of the myelin lamellae. Transmission electron microscopy showed that club-shaped Ruffini endings contained fewer mitochondria. Thus, it is possible that the club-shaped Ruffini endings in the PDL of old-aged control mouse incisors receive little if any masticatory force. The club-shape may be a morphology of Ruffini endings resulting from age- or growth-related partial or total loss of stimulation by masticatory force.

Clinically, a forward shift of the mandible is observed in patients with incisor interference. The mice in the present experimental groups exhibited this characteristic after the long-term induction of anterior crossbite. Therefore, their chewing patterns are likely to have adapted to avoid such interference. In the experimental

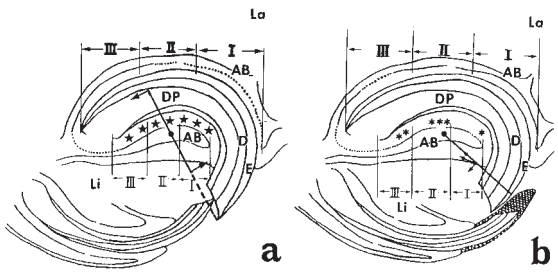

Figure 10 The possible directions of force transferred from the mandibular to the maxillary incisor during mastication in the control group (a) and the anterior crossbite group (b) as determined from the histochemical reactions for TRAP activity (dotted areas). To simplify the evaluation, both labial (La) and lingual (Li) alveolar bone (AB) were divided into a marginal (I), middle (II), and basal thirds (III). (a) The force is in an upward direction (long arrow), resulting in a counterclockwise rotation of the maxillary incisor. All of the areas of the lingual PDL are in a state of physiological tension (*). (b) The force is directed backward (long arrow). The lingual PDL may be found in one of the following three modes: pressure in the marginal third (*), abnormal tension in the basal third (**), and partial or total lack of masticatory force in the middle third (***). See text for descriptions. D, dentine; DP, dental pulp; E, enamel.

groups, the width of the marginal third of the lingual PDL was relatively decreased (Table 2), whereas that of the basal third was increased (Table 2). In addition, TRAP histochemistry clearly showed that the marginal third of the lingual PDL in the experimental groups, particularly in those beyond 6 weeks post-attachment of the appliance, was associated with non-physiological pressure, while the other areas were associated with unusual tension. This implies that during the chewing cycle in mice in the experimental groups, masticatory force is transferred to the maxillary incisors in a backward direction, probably with downwards and up-and-backwards vector elements (Figure 10b).

Sodeyama *et al.* (1996) reported that Ruffini endings showed acute responses to non-physiological mechanical stimulation of rat molars until the sixth day after the induction of occlusal trauma, and that the morphology of these Ruffini endings then seemed to recover on the seventh day, even though the appliance used to induce occlusal trauma was still attached to the occlusal surface of the rat molars. In contrast, this study revealed that nerve endings exhibited biological responses as early as the third day and could be seen until the eighth week post-attachment of the appliance.

During post-natal development, Ruffini endings formed *de novo* in rat lingual PDL exhibit rough and irregular contours, due to their cytoplasmic processes (about 1 μm long), associated with occlusal function (Nakakura *et al.*, 1993, 1995). After responding acutely to stimulation by non-physiological force caused by induced anterior crossbite, the axon terminals of Ruffini endings also showed swollen and hazy contours and unusually long (about 2 μm) finger-like projections, comparable to those described previously by Sodeyama *et al.* (1996). On the other hand, the long-term induction of anterior crossbite led to the appearance of club-shaped nerve terminations with few if any micro-projections on their surface. Excessive force due to orthodontic tooth movement produces not only hyalinization of the PDL and extensive bone resorption (Rygh and Brudvik, 1995), but also nerve injury (Loescher *et al.*, 1993; Long *et al.*, 1996). Acute morphological changes in Ruffini endings may be transient manifestations of nerve injury. The club-shaped deformation of Ruffini endings seen in chronic experiments may represent atrophic changes due to the lack of physiological stimuli, since identical club-shaped Ruffini endings were also seen in the PDL of old-aged control mouse incisors.

Ruffini endings are generally believed to be sensitive to the tension of collagenous fibres (Chambers *et al.*, 1972; Biemesderfer *et al.*, 1978). The finger-like projections or axonal spines extending from the axon terminals are involved in mechanoreception (Byers, 1985). Alterations in the morphology of nerve endings cannot be absolutely extrapolated to the physiological changes in mechanoreception. Nevertheless, the possibility that the partial or total loss of finger-like projections, as well as mitochondria and other organelles, from axon terminals might affect mechanoreception in patients with anterior crossbite, if similar changes also occur in humans, cannot be excluded.

The present results illustrate that a change in the direction of the force applied to the PDL leads to rapid and prolonged changes in the morphology of Ruffini-like mechanoreceptors.

Address for correspondence

Thosapol Piyapattamin
First Department of Orthodontics
Faculty of Dentistry
Tokyo Medical and Dental University
1–5–45 Yushima, Bunkyo-ku
Tokyo 113–8549, Japan

Acknowledgement

We are very grateful to Dr Noriko Osumi for her advice on the immunohistochemical technique.

References

Beertsen W 1975 Migration of fibroblasts in the periodontal ligament of the mouse incisor as revealed by autoradiography. Archives of Oral Biology 20: 659–666

Bhaskar S N (ed) 1986 Maxilla and mandible (alveolar process). Orban's oral histology and embryology. C V Mosby Company, St Louis, pp. 232–252

Biemesderfer D, Munger J B, Bubner R 1978 The pilo-Ruffini complex: a non-sinus hair and associated slowly-adapting mechanoreceptor in primate facial skin. Brain Research 142: 197–222

Byers M R 1985 Sensory innervation of periodontal ligament of rat molars consists of unencapsulated Ruffini-like mechanoreceptors and free nerve endings. Journal of Comparative Neurology 231: 500–518

Cash R M, Linden R W A 1982 The distribution of mechanoreceptors in the periodontal ligament of the mandibular canine tooth of the cat. Journal of Physiology 330: 439–447

Chambers M R, Andres M, During V, Iggo A 1972 Structure and function of the slowly adapting type II mechanoreceptor in hair skin. Quarterly Journal of Experimental Physiology and Cognate Medical Sciences 57: 417–445

Doran J F, Jackson P J, Kynoch P A M, Thompson R J 1983 Isolation of PGP 9.5, a new human neuron specific protein detected by high-resolution two-dimensional electrophoresis. Journal of Neurochemistry 40: 1542–1547

Egermark-Eriksson I, Ingervall B, Carlsson G E 1983 The dependence of mandibular dysfunction in children on functional and morphologic malocclusion. American Journal of Orthodontics 83: 187–194

Fristad I, Heyeraas K J, Kvinnsland I 1994 Nerve fibres and cells immunoreactive to neurochemical markers in developing rat molars and supporting tissues. Archives of Oral Biology 39: 633–646

Gulbenkian S, Wharton J, Polak J M 1987 The visualization of cardiovascular innervation in the guinea pig using antiserum to protein gene product 9.5 (PGP 9.5). Journal of Autonomic Nervous System 18: 235–247

Hiiemäe K M 1967 Masticatory function in the mammals. Journal of Dental Research 46 (Supplement 5): 883–893

Kamata S 1994 Reflex response of temporal muscle induced by mechanical stimulation to periodontal ligament—in the lateral jaw movement during mastication. Journal of the Japanese Stomatological Society 61: 82–97

Kato J, Tanne K, Ichikawa H 1992 Distribution of calcitonin gene-related peptide and substance P-immunoreactive nerve fibers and their correlation in the periodontal ligament of the mouse incisor. Acta Anatomica 145: 101–105

Kitamura E, Takashima F, Miyauchi S, Maruyama T 1987 The effect of anterior crossbite on stomatognathic function. Nippon Hotetsu Shika Gakkai Zasshi 31: 1216–1226

Kvinnsland I, Kvinnsland S 1990 Changes in CGRP immunoreactive nerve fibres during experimental tooth movement in rats. European Journal of Orthodontics 12: 320–329

Lee S K, Goldring S R, Lorenzo J A 1995 Expression of the calcitonin receptor in bone marrow cell cultures and in bone: a specific marker of the differentiated osteoclast that is regulated by calcitonin. Endocrinology 136: 4572–4581

Linden R W 1990 Periodontal mechanoreceptors and their functions. In: Taylor A (ed.) Neurophysiology of the jaws and teeth. Macmillan Press, London, pp. 52–95

Linden R W A, Millar B J 1988 The response characteristics of mechanoreceptors related to their position in the cat canineperiodontal ligament. Archives of Oral Biology 33: 51–56

Linden R W A, Millar B J, Halata Z 1994 A comparative physiological and morphological study of periodontal ligament mechanoreceptors represented in the trigeminal ganglion and the mesencephalic nucleus of the cat. Anatomy and Embryology 190: 127–135

Linden R W A, Millar B J, Scott B J J 1995 The innervation of the periodontal ligament. In: Berkovitz B K B, Moxham B J, Newman H N (eds) The periodontal ligament in health and disease. Pergamon Press, Oxford, pp. 133–159

Loescher A R, Al-Emran S, Sullivan S, Robinson P P 1993 Characteristics of periodontal mechanoreceptors supplying cat canine teeth which have sustained orthodontic forces. Archives of Oral Biology 38: 51–56

Long A, Loescher A R, Robinson P P 1996 A histological study on the effect of different periods of orthodontic force on the innervation and dimensions of the cat periodontal ligament. Archives of Oral Biology 41: 799–808

Maeda T, Osamu S, Kobayashi S, Iwanaga T, Fujita T 1989 The ultrastructure of Ruffini endings in the periodontal ligament of rat incisors with special reference to the terminal Schwann cells (K-cells). Anatomical Record 223: 95–103

Maeda T, Sato O, Kannari K, Takagi H, Iwanaga T 1991 Immunohistochemical localization of laminin in the periodontal Ruffini endings of rat incisors: a possible function of terminal Schwann cells. Archives of Histology and Cytology 54: 339–348

Malathi S, Batmanabane M 1983 Effects of varying periods of immobilization of a limb on the morphology of a

peripheral nerve. Acta Morphologica Neerlando-Scandinavica 21: 185–198

Matthews B 1975 Mastication. In: Lavelle C L B (ed.) Applied physiology of the mouth. John Wright, Bristol, pp. 199–242

Minkin C 1982 Bone acid phosphatase: tartrate-resistant acid phosphatase as a marker of osteoclast function. Calcified Tissue International 34: 285–290

Mohlin B, Kopp S 1978 A clinical study of the relationship between malocclusions, occlusal interferences and mandibular pain and dysfunction. Swedish Dental Journal 2: 105–112

Nakakura O K, Maeda T, Sato O, Takano Y 1993 Postnatal development of periodontal innervation in rat incisors: an immunohistochemical study using protein gene product 9.5 antibody. Archives of Histology and Cytology 56: 385–398

Nakakura O K, Maeda T, Ohshima H, Noda T, Takano Y 1995 Postnatal development of periodontal Ruffini endings in rat incisors: an immunoelectron microscopic study using protein gene product 9.5 antibody. Journal of Comparative Neurology 362: 551–564

Proffit W R (ed.) 1993 The etiology of orthodontics problems. Contemporary orthodontics. C V Mosby Company, St Louis, pp. 105–136

Proffit W R, Fields H W 1993 Orthodontic treatment planning: from problem list to specific plan. In: Proffit W R (ed.) Contemporary orthodontics. C V Mosby Company, St Louis, pp. 186–224

Ramieri G *et al.* 1990 The innervation of human teeth and gingival epithelium as revealed by means of an antiserum for protein gene product 9.5. American Journal of Anatomy 189: 146–154

Reitan K 1985 Biomechanical principles and reactions. In: Graber T M, Swain B F (eds) Orthodontics: current principles and techniques. C V Mosby Company, St Louis, pp. 101–192

Rugh R (ed) 1967 Tooth development. In: The mouse—its reproduction and development. Burgess Publishing Company, Minnesota, pp. 227–236

Rygh P, Brudvik P 1995 The histological responses of the periodontal ligament to horizontal orthodontic loads. In: Berkovitz B K B, Moxham B J, Newman M N (eds) The periodontal ligament in health and disease. Pergamon, Oxford, pp. 243–258

Sato O *et al.* 1988 Innervation of periodontal ligament and dental pulp in the rat incisor: an immunohistochemical investigation of neurofilament protein and glia-specific S-100 protein. Cell and Tissue Research 251: 13–21

Sato O, Maeda T, Toshihiko I, Kobayashi S 1989 Innervation of the incisors and PDL in several rodents: an immunohistochemical study of neurofilament protein and glia-specific S-100 protein. Acta Anatomica 134: 94–99

Schmechel D, Marangos P J, Brightman M 1978 Neurone-specific enolase is a molecular marker for peripheral and central neuroendocrine cell. Nature 276: 834–836

Schour I, Massler M 1962 The teeth. In: Farris E J, Griffith J Q (eds) The rat in laboratory investigation. Hanfner Publishing Company, New York, pp. 104–165

Shore R C, Berkovitz B K B 1978 Model to explain differential movement of periodontal fibroblasts. Archives of Oral Biology 23: 507–509

Sodeyama T, Maeda T, Takano Y, Hara K 1996 Responses of periodontal nerve terminals to experimentally induced occlusal trauma in rat molars: an immunohistochemical study using PGP 9.5 antibody. Journal of Periodontal Research 31: 235–248

Thompson R J, Doran J F, Jackson P, Shillon A P, Rode J 1983 PGP 9.5—a new marker for vertebrate neurons and neuroendocrine cells. Brain Research 278: 224–228

Tsuchiya T, Matsumoto Y, Kurihara S 1995 The fluorescent simultaneous azo dye technique for demonstration of tartrate-resistant acid phosphatase (TRAP) activity in osteoclast-like multinucleate cells. Journal of Bone and Mineral Metabolism 13: 71–76

Urena P, Hruby M, Ferreira A, Ang K S 1996 Plasma total versus bone alkaline phosphatase as markers of bone turnover in hemodialysis patients. Journal of the American Society of Nephrology 7: 506–512